

Numerical simulation of turbulent propane-air combustion with non-homogeneous reactants: initial results

By D. Haworth,¹ B. Cuenot,² T. Poinsot,³ AND R. Blint¹

High-resolution two-dimensional numerical simulations have been initiated for premixed turbulent propane-air flames propagating into regions of non-homogeneous reactant stoichiometry. Simulations include complex chemical kinetics, realistic molecular transport, and fully resolved hydrodynamics (no turbulence model). Aero-thermochemical conditions (pressure, temperature, stoichiometry, and turbulence velocity scale) approach those in an automotive gasoline direct-injection (GDI) engine at a low-speed, light-load operating condition. Initial results suggest that: 1) There is no leakage of the primary fuel (propane) behind an initial thin premixed heat-release zone. This 'primary premixed flame' can be described using a monotonic progress variable and laminar premixed flamelet concepts. 2) Following an initial transient, global heat release with non-homogeneous reactants is lower than with homogeneous reactants for the same overall reactant stoichiometry. Flame area (length) is greater with non-homogeneous reactants. 3) Beyond three-to-four flame thicknesses behind the primary flame, practically all hydrocarbon fuel has broken down into CO and H₂. 4) The rate of heat release in the 'secondary reaction zone' behind the primary premixed flame is governed by turbulent mixing and the kinetics of CO₂ production. Mixture-fraction-conditioned secondary heat release, CO, and CO₂ production rates are qualitatively similar to results from a first-order conditional-moment-closure (CMC) model; CMC gives poor results for H₂, H₂O, and radical species. Description of the secondary heat release using simple laminar diffusion flamelet concepts is problematic. 5) Computational considerations demand modifications to chemical mechanisms involving C₃H₇ and CH₃CO. Specific changes are proposed to strike a satisfactory balance between accuracy and computational efficiency over a broad range of reactant stoichiometry.

1. Introduction

Stratification of the in-cylinder fuel-air mixture has the potential to reduce significantly the fuel consumption of automotive reciprocating internal-combustion (IC) engines. As a result, both spark-ignition gasoline (Lai *et al.* 1997) and compression-ignition Diesel (Krieger *et al.* 1997) direct-injection engines currently are subjects

1 GM R&D Center, Warren, MI

2 Centre Européen de Recherche et de Formation Avancée en Calcul Scientifique, Toulouse

3 Institut de Mécanique des Fluides de Toulouse, Toulouse

of intense research. In a direct-injection engine, liquid fuel is injected directly into the combustion chamber to generate a highly non-homogeneous fuel/air/residual mixture at the time of ignition and flame propagation.

The motivation for the present research is to determine the effects of reactant stratification on turbulent flame propagation, and to incorporate this new understanding into turbulent combustion models. The application of interest is the gasoline direct-injection (GDI) engine. Specifically, we seek: 1) to validate or invalidate a conceptual framework initially adopted for modeling this combustion regime (Fig. 1); 2) to quantify differences in the primary heat release process between homogeneous and non-homogeneous reactants; and 3) to determine the chemical composition and heat-release rates for the fuel fragments and oxidizer that penetrate behind the primary heat-release zone.

The tool selected is high-fidelity numerical simulation including turbulence, complex chemical kinetics, and full multi-component molecular transport. Propane-air ($\text{C}_3\text{H}_8/\text{O}_2/\text{N}_2$ reactants) is the simplest hydrocarbon system that exhibits chemical behavior, laminar flame speeds and thicknesses, and extinction limits that are comparable to those of heavier paraffin fuels (Turns 1996). It is probably the smallest system from which quantitative information directly relevant to the oxidation of heavier liquid gasoline and Diesel fuels can be extracted, and is therefore an appropriate choice for this study.

In addition to addressing specific physics and modeling issues, this work also advances the state-of-the-art in ‘direct’ numerical simulation of turbulent combustion (*i.e.*, computations in which all spatial and temporal scales are resolved without filtering or turbulence modeling). Simulation is extended to detailed propane-air chemistry and transport and to high pressure and temperature reactants with extreme fuel-lean and fuel-rich stoichiometry. Propane-air chemical kinetics is based on a 29-species, 73-reaction mechanism originally published by Warnatz (1981) and subsequently modified and extended to IC-engine conditions by Blint (1988, 1991). Modifications to reaction steps involving C_3H_7 and CH_3CO are introduced for computational practicality. The chemical mechanism is implemented in the numerical code NTMIX-CHEMKIN (Baum 1994), which has been used in a number of earlier numerical turbulent combustion studies including hydrogen-oxygen flames (Baum *et al.* 1994) and methane-air systems (Hilka *et al.* 1995). The formulation is similar to that used by other researchers for turbulent hydrogen-air (Im *et al.* 1998) and methane-air (Gran *et al.* 1996; Chen & Im 1998) combustion. Earlier numerical studies of turbulent premixed flames with non-homogeneous reactants have used one-step irreversible chemistry (Poinsot *et al.* 1996; Hélie and Trouvé 1998) and have focused on the primary premixed burn. Here secondary reaction (heat release occurring behind the primary flame) is emphasized.

2. Stratified Turbulent Combustion in a GDI Engine

2.1 Combustion regime

Many of the combustion issues to be resolved in GDI automotive engines arise during low-speed light-load operation. At 2,000 r/min and 330 kPa NMEP (net

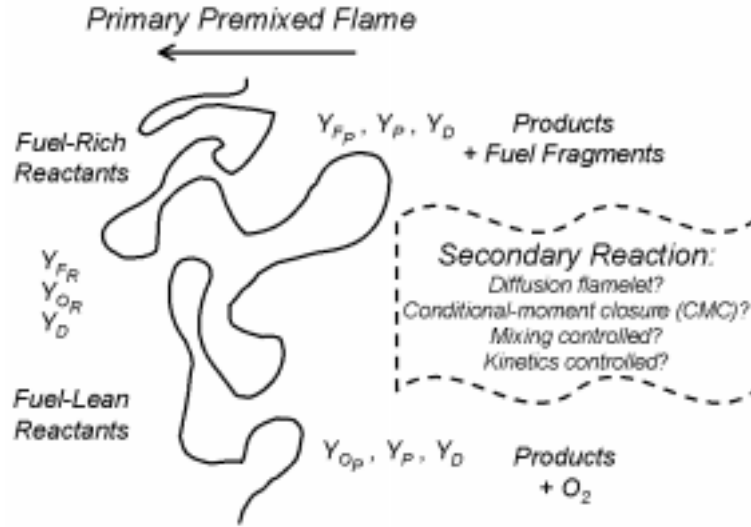


FIGURE 1. A schematic of turbulent flame propagation into a region of non-homogeneous reactants. The six mass fractions Y_α correspond to the six streams defined in the skeletal combustion model of Eqs. (1) and (2).

mean effective pressure), the in-cylinder fuel/air mixture is globally fuel-lean. A typical overall fuel-based equivalence ratio is $\Phi \approx 0.3$, where Φ is reactant fuel-to-air mass ratio, divided by the stoichiometric fuel-to-air mass ratio (Section 3.4). Moreover, the mixture remains highly non-homogeneous at the time of ignition. The local equivalence ratio ranges from below the lean flammability limit ($\Phi \approx 0.5$) to above the rich flammability limit ($\Phi \approx 3$) over a distance of less than one centimeter. The in-cylinder pressure and temperature at time of ignition are approximately four atmospheres and 700 K, respectively. Global turbulence rms velocity u'_T and integral length scale l_T are estimated based on a number of experimental measurements and computational studies (Haworth & Poinso 1992): $u'_T \approx 6$ m/s and $l_T \approx 2$ -4 mm.

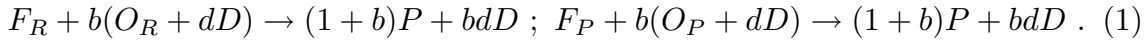
The mixture is ignited via spark discharge at a location where the local equivalence ratio is close to unity. At four atmospheres and 700 K, a stoichiometric premixed laminar flame propagates at about 1.6 m/s (the steady unstrained laminar flame speed, s_l^0) and has a thickness of about 0.1 mm (the laminar flame thickness based on maximum temperature gradient, δ_l^0). The initially healthy propagating turbulent premixed flame soon encounters fuel-rich and fuel-lean extremes in reactant stoichiometry.

The turbulent combustion regime is characterized by comparing turbulence (hydrodynamic) scales with laminar-flame (chemical) scales. Either velocity- and length-scale ratios or equivalently, Reynolds and Damköhler numbers, can be used. Values corresponding to this engine example are $u'_T/s_l^0 \approx 4$ and $l_T/\delta_l^0 \approx 20 - 40$ ($Re_T \equiv u'_T l_T/\nu \approx 600 - 1,200$ and $Da \equiv (l_T/u'_T) \cdot (s_l^0/\delta_l^0) \approx 5 - 10$). The parameter range corresponding to the rotational speeds, loads, and dilution levels of interest in IC engines is $u'_T/s_l^0 \approx 0.5 - 20$ and $l_T/\delta_l^0 \approx 3 - 50$ (Haworth & Poinso 1992). It

is flame propagation into spatially varying reactant stoichiometry in this parameter range that we seek to understand and to model. Of primary interest is the rate at which chemical energy is converted to sensible energy (heat).

2.2 A conceptual framework for modeling heat release

We hypothesize a two-stage combustion process (Fig. 1). Fuel and oxidizer are well mixed at the molecular level in the unburned reactants, but the mixture composition is spatially non-uniform. Fuel and oxidizer initially react to release heat and form product in a primary premixed flame. Behind the premixed flame are hot combustion products. In locally fuel-rich regions, excess fuel or fuel fragments pass through the primary flame; in locally fuel-lean regions, there is excess oxidizer behind the primary flame. Secondary heat release occurs as the post-flame fuel (or fuel fragments) and oxidizer mix at the molecular level and react. A skeletal model is constructed to provide a conceptual basis for analysis (El Tahry 1997). We consider six ‘streams:’ (1) ‘reactant’ fuel Y_{FR} - that is, fuel in front of the primary premixed flame; (2) reactant oxidizer Y_{OR} ; (3) ‘product’ fuel Y_{FP} ; (4) product oxidizer Y_{OP} ; (5) combustion product Y_P ; and (6) inert diluent Y_D . We denote by b the stoichiometric mass of oxidizer per unit mass of fuel and by d the mass of diluent per unit mass of oxidizer. The overall reaction then can be represented on a per-unit-mass-of-fuel basis as,



The turbulent combustion model comprises partial differential equations (pde’s) for the mean mass fractions $\langle Y_\alpha \rangle$, $\alpha = 1, \dots, 6$. An equation for the mean enthalpy $\langle h \rangle$ and auxiliary relations (*e.g.*, fluid properties; Kee *et al.* 1983) also are needed. Here and in the following, angled brackets $\langle \rangle$ denote ensemble mean quantities. Pde’s for the mean mass fractions have the form:

$$\begin{aligned} \frac{D\rho\langle Y_{FR} \rangle}{Dt} &= D_{FR} - R_{FR \rightarrow P} - S_{FR \rightarrow FP} ; & \frac{D\rho\langle Y_{OR} \rangle}{Dt} &= D_{OR} - bR_{FR \rightarrow P} - S_{OR \rightarrow OP} ; \\ \frac{D\rho\langle Y_{FP} \rangle}{Dt} &= D_{FP} - R_{FP \rightarrow P} + S_{FR \rightarrow FP} ; & \frac{D\rho\langle Y_{OP} \rangle}{Dt} &= D_{OP} - bR_{FP \rightarrow P} + S_{OR \rightarrow OP} ; \\ \frac{D\rho\langle Y_P \rangle}{Dt} &= D_P + (1 + b)R_{FR \rightarrow P} + (1 + b)R_{FP \rightarrow P} ; & \frac{D\rho\langle Y_D \rangle}{Dt} &= D_D . \end{aligned} \quad (2)$$

Here D/Dt denotes a material derivative following the mean fluid velocity and D_α is an effective (laminar-plus-turbulent) diffusion term. Reaction source terms $R_{FR \rightarrow P}$ and $R_{FP \rightarrow P}$ are the rates at which reactant and product fuel, respectively, are converted to combustion product. Terms $S_{FR \rightarrow FP}$ and $S_{OR \rightarrow OP}$ are the rates at which reactant fuel and oxidizer, respectively, are converted to product fuel and oxidizer without participating in the primary heat release. These account for locally fuel-rich or fuel-lean reactants, and phenomena including local quenching of the primary flame or vaporization of liquid fuel that occurs behind the primary flame.

2.3 Modeling issues

In this preliminary report, we limit our attention to the reaction source terms.

2.3.1 Primary heat release

We consider first the primary flame ($R_{F_R \rightarrow P}$). Here the goal is to determine to what extent existing models for homogeneous turbulent premixed combustion must be modified to account for reactant stratification (assuming, for the moment, that they remain appropriate at all). Laminar premixed flamelet models have proven successful in modeling the overall heat-release rate in homogeneous-charge IC engines. For example, a model developed by El Tahry (1990) has been applied to practical engine configurations (Khalighi *et al.* 1995). In this model, the reaction source term is written as $R_{F_R \rightarrow P} = \rho_u \langle Y_{F_R} \rangle \gamma \langle s_l / \delta_l \rangle$, where ρ_u is the unburned gas density, s_l is a laminar flame speed, δ_l is a laminar flame thickness, and γ is the probability of encountering an active reaction zone. Equivalently, one can write $R_{F_R \rightarrow P} = \rho_u \langle Y_{F_R} \rangle \langle s_l \rangle \Sigma$, where Σ is the flame surface-to-volume ratio (*e.g.*, Boudier *et al.* 1992).

Important issues include the time evolution of flame area (γ or Σ), the global heat release rate for non-homogeneous reactants compared to those for homogeneous reactants having the same overall stoichiometry, and determination of the extent to which the local structure of the primary premixed flame differs from that of a steady one-dimensional laminar flame under the same thermochemical conditions.

2.3.2 Secondary reaction

It is less clear how to proceed in modeling the secondary heat release ($R_{F_P \rightarrow P}$). One-step irreversible chemistry (fuel+oxidizer \rightarrow product) implies that either fuel or oxidizer must be depleted on passing through the primary flame (Poinsot *et al.* 1996; Hélie & Trouvé 1998). However, in a hydrocarbon-air system, the fuel might be partially or completely broken down into smaller fragments, all species are present in non-zero concentrations behind the primary flame, and each species diffuses at a different rate—resulting, for example, in segregation of hydrogen-containing and carbon-containing species that originated in the fuel.

Important questions related to the secondary combustion include: Is there any leakage of fuel (propane) behind the primary flame? What is the composition of fuel fragments behind the primary flame? What is the rate-controlling process governing secondary heat release and what type of turbulent combustion model is most appropriate (*e.g.*, chemical-kinetics-controlled versus turbulent-mixing-controlled versus laminar-diffusion-flamelet versus conditional-moment-closure (CMC) models)?

3. The model problem

3.1 Governing equations and configuration

The system considered is a compressible multi-component reacting ideal-gas mixture. Principal equations express conservation of mass (mixture density ρ), linear momentum (mixture velocity \underline{u}), N_S chemical species (mass fractions Y_α , $\alpha = 1, \dots, N_S$), and energy (total energy density e_t). Chemical production terms are

expressed in Arrhenius form, and species molecular transport is modeled using a multicomponent form of Fick's law. Soret and Dufour effects are not included. All fluid properties, molecular transport coefficients, and chemical production terms are computed using the CHEMKIN and TRANSPORT packages (Kee *et al.* 1980, 1983). The full system of governing equations and assumptions can be found in Baum (1994) and Baum *et al.* (1994).

Here the focus is on chemical reaction source terms. The pde governing the evolution of species mass fraction Y_α is,

$$\frac{\partial \rho Y_\alpha}{\partial t} + \frac{\partial \rho Y_\alpha u_j}{\partial x_j} = - \frac{\partial \rho Y_\alpha V_{\alpha j}}{\partial x_j} + W_\alpha \dot{\omega}_\alpha, \quad (3)$$

where $\dot{\omega}_\alpha$ is the molar chemical production rate of species α and W_α is its molecular weight. The quantity $V_{\alpha j}$ is the diffusion velocity (j^{th} Cartesian component) for species α . In terms of species production rates and formation enthalpies $\Delta h_{f\alpha}^0$, the heat-release rate $\dot{\omega}_Q$ (the rate of conversion from chemical to sensible enthalpy) is,

$$\dot{\omega}_Q = - \sum_{\alpha=1}^{N_S} \dot{\omega}_\alpha \Delta h_{f\alpha}^0. \quad (4)$$

All chemical source terms are specified functions of the local mixture composition and temperature (Section 3.2): $\dot{\omega}_\alpha = \dot{\omega}_\alpha(\underline{Y}, T)$; $\dot{\omega}_Q = \dot{\omega}_Q(\underline{Y}, T)$. The pressure is approximately uniform.

The governing equations are solved in a Cartesian frame of reference using sixth-order compact finite-differences (Lele 1992) for spatial derivatives and third-order Runge-Kutta time integration. Computational considerations preclude carrying out spatially three-dimensional simulations with realistic chemistry and transport in the parameter range of interest. The available options are: spatially two-dimensional computations with detailed chemistry and transport for hydrodynamic scales approaching relevant values; or spatially three-dimensional computations with simple chemistry and transport at lower Re and Da . To address the issues of interest here, we have chosen the former.

Calculations are initialized with reactants on one side of the computational domain and products on the other; these are separated by a stoichiometric planar laminar premixed flame. The initial flame is a steady one-dimensional solution to the full set of governing equations. Initially isotropic two-dimensional turbulence is prescribed using a two-parameter turbulence energy spectrum $E(k)$ (Haworth & Poinsot 1992). The parameters correspond to the initial rms turbulence velocity u'_{T_0} and to the wavenumber of the spectrum peak k_{max} . Here the product $\rho u'_{T_0}$ is uniform through the flame, so that the rms turbulence level u'_{T_0} is higher in the hot burned products than in the cooler reactants. The initial turbulence integral length scale l_{T_0} corresponds to $l_{T_0} \approx 0.3 \cdot \frac{2\pi}{k_{max}}$. On lateral boundaries, periodic conditions are enforced while non-reflecting boundary conditions are used on inflow/outflow boundaries.

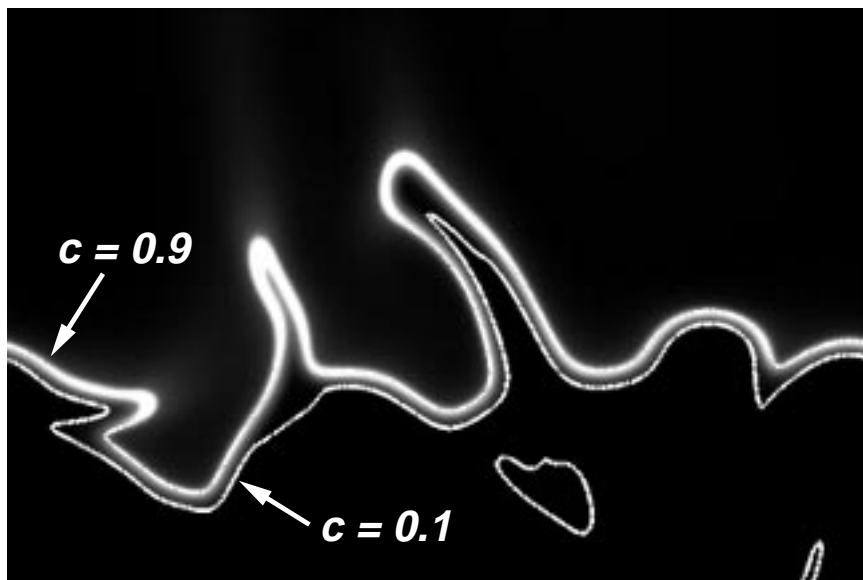


FIGURE 2. Computed two-dimensional heat-release field for homogeneous stoichiometric reactants (Table I) at time $t/\tau_f = 3.5$. Black corresponds to minimum heat release (0.0) and white to maximum (0.36). Iso-contours of reaction progress variable (white lines: $c = 0.1$ and $c = 0.9$, Eq. 8) are superposed. The $c = 0.9$ iso-contour is close to the peak heat release.

Reactant non-homogeneity is introduced by varying the mass fractions of C_3H_8 , O_2 , and N_2 in the reactants. This is done in a manner that maintains the same total quantity of fuel and oxidizer as for a baseline homogeneous stoichiometric case, and maintains a uniform ratio of N_2 to O_2 (uniform air composition). Here we consider a large-scale sinusoidal non-homogeneity where the variation in composition parallel to the initially planar flame (the periodic y direction) is of the form $\sin(2\pi y/L_y)$, L_y being the y -direction length of the computational domain. The equivalence ratio ranges from a minimum at $y = 0$ and $y = L_y$ to a maximum at $y = L_y/2$. The time required for the change in reactant stoichiometry to penetrate the primary premixed flame is estimated as,

$$\tau_f = 2\delta_l^0 / (s_l^0(1 + \rho_u/\rho_b)) . \quad (5)$$

Here ρ_u and ρ_b refer to the unburned- and burned-gas mass density, respectively. This chemical flame time accounts for the acceleration of gases as they pass from the cooler reactants to the hotter products. To explore secondary reaction, it is anticipated that one must integrate to times on the order of several τ_f 's.

Key aerothermochemical parameters for the two cases considered in this report are summarized in Table I. Reactant composition, temperature, and pressure are selected to match the engine condition of Section 2.1. The initial rms turbulence level is within the range of interest in IC-engine combustion. However, the turbulence integral length scale is low by a factor of ten. This is, in part, a consequence of the small box size chosen for these initial runs. The computed heat-release field of Fig. 2 serves to illustrate the configuration.

3.2 Base propane-air mechanism

The base 29-species 73-reaction chemical mechanism (Warnatz 1981; Blint 1988, 1991) will be referred to as mechanism *M1*. Mechanism *M1* has been validated against available experimental measurements of laminar flame speed for ambient-pressure-and-temperature reactants (Blint & Tsai 1998). It has been used to explore in-cylinder engine combustion issues including dilution (Blint 1988) and stretch (Blint 1991) effects, and has been used to generate a laminar flame library (Blint & Tsai 1998) that has been coupled with a turbulent combustion model similar to that of Section 2.2 and applied both to homogeneous and non-homogeneous spark-ignited combustion in practical engine configurations. For present purposes, nitrogen is treated as an inert diluent. In all computations, reactant air is defined on a volume basis as 21% O₂, 79% N₂ ($(Y_{N_2}/Y_{O_2})_{\text{reactants}} = 3.25$).

Table I. Parameters for initial *M2* homogeneous-reactant and non-homogeneous-reactant cases. Pressure is four atmospheres, reactant temperature is 700 K, and the global reactant equivalence ratio is unity.

Case	L_x/n_x	L_y/n_y	Φ_{min}/Φ_{max}	$\frac{\tau_f}{\tau_{T0}}$	$\frac{u'_{T0}}{s'_{\phi=1}}$	$\frac{l_{T0}}{\delta'_{\phi=1}}$	Re_{T0}
Homogeneous	2 mm/301	3 mm/451	1.0/1.0	0.92	3.8	1.8	71
Non-homogeneous	2 mm/301	3 mm/451	0.0/4.0	0.92	3.8	1.8	71

3.3 Modified chemical mechanisms

The maximum allowable computational time step and mesh spacing are determined, respectively, by the shortest time and length scales encountered in solving the coupled set of governing pde's. In the absence of chemical reaction, the smallest hydrodynamic length scale to be resolved is the Kolmogorov turbulence microscale. In that case, the time step for the fully compressible numerical methodology is limited by a CFL condition based on the local sound speed: $\Delta t < \Delta x/a$, where $a = (kRT)^{1/2}$ ($k \equiv c_p/c_v$, the ratio of specific heats; R is the specific gas constant). Chemical reaction introduces additional time and length scales. For a stoichiometric four-atmosphere propane-air flame, mechanism *M1* requires a computational time step that is nearly 1,000 times smaller than the CFL limit.

Clearly, a judicious reduction of the chemical mechanism is needed. A modified mechanism *M2* incorporates two changes to *M1* that together return the time-step limitation to a CFL condition: two of the rate-limiting species C₃H₇(N) and C₃H₇(I) are removed; and an equilibrium assumption is introduced for the remaining rate-limiting species CH₃CO. Rate coefficients in several reaction steps are adjusted accordingly.

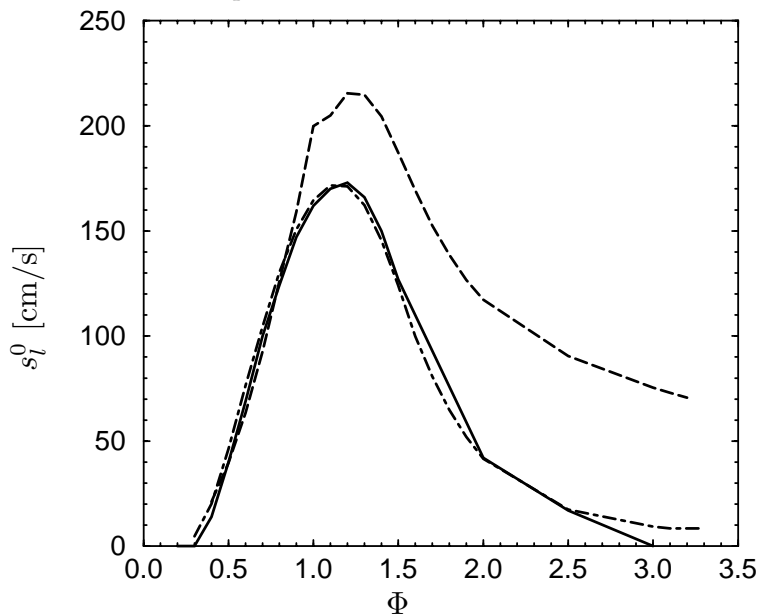


FIGURE 3. Computed variation of steady unstrained laminar flame speed s_l^0 with equivalence ratio Φ at four atmospheres for 700 K reactants. Results are shown for three versions of the propane-air chemical mechanism: — $M1$; ---- $M2$; -.- $M3$.

The changes from $M1$ to $M2$ degrade the mechanism’s performance on the fuel-rich side of stoichiometric. Fig. 3 shows computed steady unstrained one-dimensional laminar flame speed as a function of equivalence ratio for four-atmosphere, 700 K reactants. The two mechanisms behave similarly on the fuel-lean side of stoichiometric; $M2$ ’s peak laminar flame speed is 23% higher than $M1$ ’s; and on the fuel-rich side, $M2$ ’s decrease in flame speed with increasing equivalence ratio is too slow: burning remains robust even at $\Phi = 3$.

A third mechanism that attempts to address the shortcomings of $M2$ on the fuel-rich side is designated as $M3$. Mechanism $M3$ retains one isomer of C_3H_7 ($C_3H_7(I)$), and includes modified rate coefficients for several related reactions. The resulting flame-speed-versus-equivalence ratio behavior is practically identical to that of $M1$ (Fig. 3). Also, CH_3CO no longer introduces a time-step-limiting time scale. Unfortunately, while $C_3H_7(I)$ is crucial to satisfactory fuel-rich behavior, it requires a time step that is about a factor of ten smaller than CFL.

At the time of this writing, work continues towards a well-balanced (accuracy versus computational efficiency) chemical mechanism, following along the lines of $M3$. In the meantime, preliminary turbulent simulations using $M2$ were initiated with the purpose of generating a ‘first look’ database for non-homogeneous turbulent propane-air flames. For these initial simulations, a $2\text{ mm} \times 3\text{ mm}$ computational domain is discretized on a 301×451 node mesh (Table I). The computational time step is limited by a sound-speed CFL condition. In spite of the known shortcomings of $M2$, extreme fuel-lean and fuel-rich stoichiometry are included. This has been done in the spirit of generating large effects that can be readily discerned, and to facilitate diagnostics development.

3.4 Diagnostics

Global quantities and primary-premixed-flame-front quantities of interest have been introduced in the course of earlier numerical studies of propagating premixed turbulent flames (Haworth & Poinsot 1992; Baum 1994; Baum *et al.* 1994; Poinsot *et al.* 1996; Hélie & Trouvé 1998). Quantities related to specific secondary-combustion models will be defined in Section 5. Here we discuss two quantities that are particularly germane to mixed-mode (premixed/non-premixed) combustion: mixture fraction and progress variable.

3.4.1 Mixture fraction

A mixture fraction field $z = z(\underline{x}, t)$ in a reacting flow quantifies the local mass fraction of material that originated from the reactant fuel (versus oxidizer or diluent); it is particularly useful in the analysis and modeling of laminar and turbulent non-premixed systems (Turns 1996). Mixture fractions are defined in such a way that they do not depend directly on chemical reaction. That is, the transport equation for $z(\underline{x}, t)$ contains no chemical source term. Element mass fractions serve for this purpose. With subscript β referring to a chemical element (one of C or H here, as there is no O or N in the propane fuel), a mixture fraction z_β is defined as,

$$z_\beta \equiv \sum_{\alpha=1}^{N_S} n_{\beta\alpha} W_\beta Y_\alpha / W_\alpha . \quad (6)$$

Here $n_{\beta\alpha}$ is the number of atoms of element β in species α , and W_β is the molecular weight of element β .

Equations (3) and (6) guarantee that the pde governing $z_\beta(\underline{x}, t)$ is free of a chemical source term. At the same time, the particular linear combination of species mass fractions that yields $\dot{\omega}_\beta \equiv 0$ cannot simultaneously cancel the diffusion term. Except in unusual cases (*e.g.*, equal and constant diffusivities for all species), z_β will vary through the reaction zone in a laminar premixed flame, even while it takes on the same value in pure reactants as in equilibrium products. Moreover, while the ratio z_C/z_H is constant in homogeneous reactants, differential diffusion causes this ratio to vary in a reacting flow.

To account for all local mass that originated in the fuel stream, a carbon-plus-hydrogen mixture fraction $z_{C+H} = z_C + z_H$ is used: in pure reactants, $z_{C+H} = Y_{C_3H_8}$. This mixture fraction reduces to that introduced for one-step irreversible chemistry by Poinsot *et al.* (1996) in their studies of non-homogeneous turbulent premixed combustion.

For a hydrocarbon-air system, reactants are said to be in *stoichiometric* proportion when there is exactly enough oxygen to oxidize all carbon in the fuel to CO_2 and all hydrogen to H_2O . For propane-air, this corresponds to five moles of oxygen per mole of fuel. Corresponding stoichiometric mixture fraction values are: $z_{C\ st} = 0.04980$; $z_{H\ st} = 0.01115$; and $z_{C+H\ st} = 0.06095$.

Closely related to mixture fraction are quantities including equivalence ratio and air-fuel ratio that are widely used in the engineering combustion community. A fuel-based equivalence ratio Φ , for example, is defined as the reactant fuel-to-air mass

ratio divided by the fuel-to-air mass ratio for stoichiometric reactants. Equivalence ratio and mixture fraction are related by,

$$\Phi = \frac{z_{C+H}}{1 - z_{C+H}} \frac{1 - z_{C+H}^{st}}{z_{C+H}^{st}}, \quad (7)$$

where it is understood that Φ is defined only in pure reactants (well ahead of the primary flame).

3.4.2 Progress variable

In the analysis and modeling of laminar or turbulent premixed flames, it is convenient to work with a quantity that increases monotonically from zero in fresh reactants to unity in fully-burned products. For quantitative work, it is necessary to associate this ‘reaction progress variable’ $c = c(\underline{x}, t)$ with specific physical quantities such as species mass fractions or temperature.

In their report on turbulent premixed flames with non-homogeneous reactants, Poinso *et al.* (1996) introduced a reaction progress variable defined in terms of local mixture fraction. Their definition was appropriate for single-step irreversible chemistry where either fuel (in fuel-lean regions) or oxidizer (in fuel-rich regions) is completely depleted in passing through the primary premixed flame. With complex chemistry, it is not clear *a priori* whether there exists any simple combination of physical variables that unambiguously marks a primary flame zone. In the present work, it is found that the primary fuel (propane) does not survive the initial heat-release zone even in locally fuel-rich regions. Following Poinso *et al.* (1996), we therefore propose the following reaction progress variable:

$$c \equiv 1 - Y_{C_3H_8} / z_{C+H}. \quad (8)$$

In unburned reactants, $z_{C+H} = Y_{C_3H_8}$ so that $c = 0$; and at any point where there is no propane, $c = 1$. The appropriateness of this choice will become clear in Section 5.

4. One-dimensional unsteady laminar premixed flames

As a prelude to two-dimensional turbulent cases, computations were performed for one-dimensional laminar premixed flames propagating into a step change in reactant stoichiometry. Two cases are considered: an initially steady stoichiometric flame propagating into fuel-lean ($\Phi = 0.5$) reactants; and an initially steady stoichiometric flame propagating into fuel-rich ($\Phi = 2.0$) reactants.

Figure 4 shows the time evolution of computed heat-release profiles (mechanism *M2*, four atmospheres, 700 K reactants). For the stoichiometric-to-lean case, peak heat release drops monotonically as the heat-release profile shifts towards the product side. The peak heat release for the steady-state $\Phi = 0.5$ laminar flame is 12% that of the stoichiometric flame.

In the stoichiometric-to-rich case (Fig. 4b), the peak heat release initially increases as the flame encounters excess fuel; it then decreases to a steady-state value that is 53% of the initial $\Phi = 1.0$ peak. The heat-release profile develops a double-peaked structure that persists to the $\Phi = 2.0$ steady state. For a stoichiometric-to-rich transient to $\Phi = 4.0$, the heat-release ‘valley’ actually becomes negative (not shown).

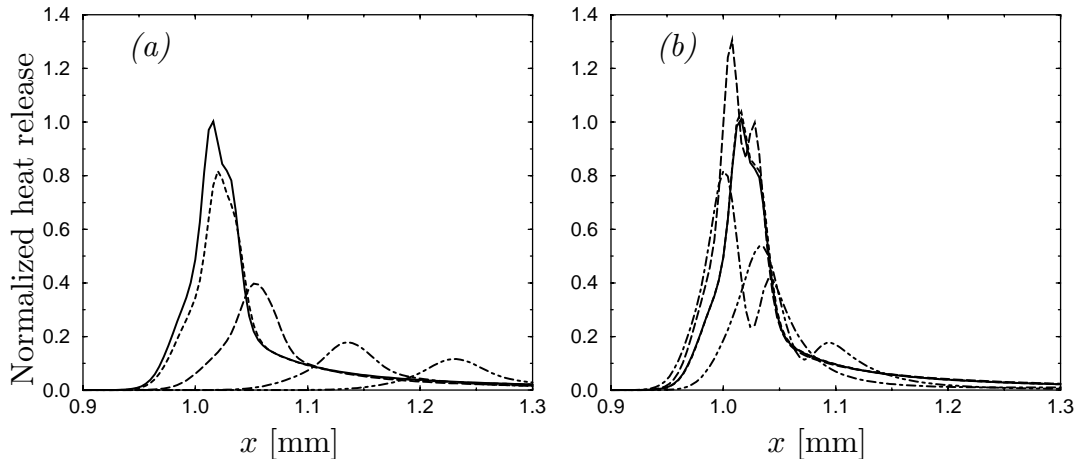


FIGURE 4. Computed heat-release profiles at several instants of time for unsteady unstrained laminar premixed propane-air flames propagating through a step change in reactant stoichiometry: four-atmosphere 700 K reactants, mechanism *M2*. Heat release is normalized by the peak value for the initial stoichiometric flame: — $t/\tau_f = 0$; $t/\tau_f = 1.4$; ---- $t/\tau_f = 4.1$; —·— $t/\tau_f = 8.2$; — — — $t/\tau_f = 12.2$. a) Stoichiometric to $\Phi = 0.5$. b) Stoichiometric to $\Phi = 2.0$.

5. Two-dimensional turbulent flames

5.1 Global observations

Results at the latest available time ($t/\tau_f = 3.5$; $t/\tau_{T0} = 3.2$) are analyzed. A single computed field (heat release) is shown for homogeneous stoichiometric reactants (Fig. 2). Isocontours of progress variable are superposed. Figure 2 illustrates visually the extent to which turbulence has perturbed the initially planar flame to increase its surface area (length) by this time.

Figure 2 can be compared to the corresponding non-homogeneous-reactant case at the same instant (Fig. 5a). The same initial ‘realization’ of a turbulent flow field has been used in both cases, and the resulting overall shapes of the primary reaction zone (progress variable iso-contours) are similar. This suggests that at early times, turbulence determines the shape of the propagating primary premixed flame sheet. At later times, it is anticipated that differences between the homogeneous and non-homogeneous flames will be greater.

Examples of several other computed fields are shown in Fig. 5 for the non-homogeneous-reactants case. Three important initial observations are made.

First, there is no leakage of propane fuel past the primary heat-release zone, even in locally fuel-rich regions. As long as the flame does not completely quench, similar behavior is expected even with improved fuel-rich mechanisms. To the extent that this conclusion is general, it largely validates the two-stage conceptual framework of Fig. 1.

Second, the disappearance of primary fuel (propane) coincides with the zone of maximum heat release. This validates the specific choice of progress variable adopted in Eq. (8) and suggests that classic premixed flamelet concepts might remain appropriate for modeling the primary heat release.

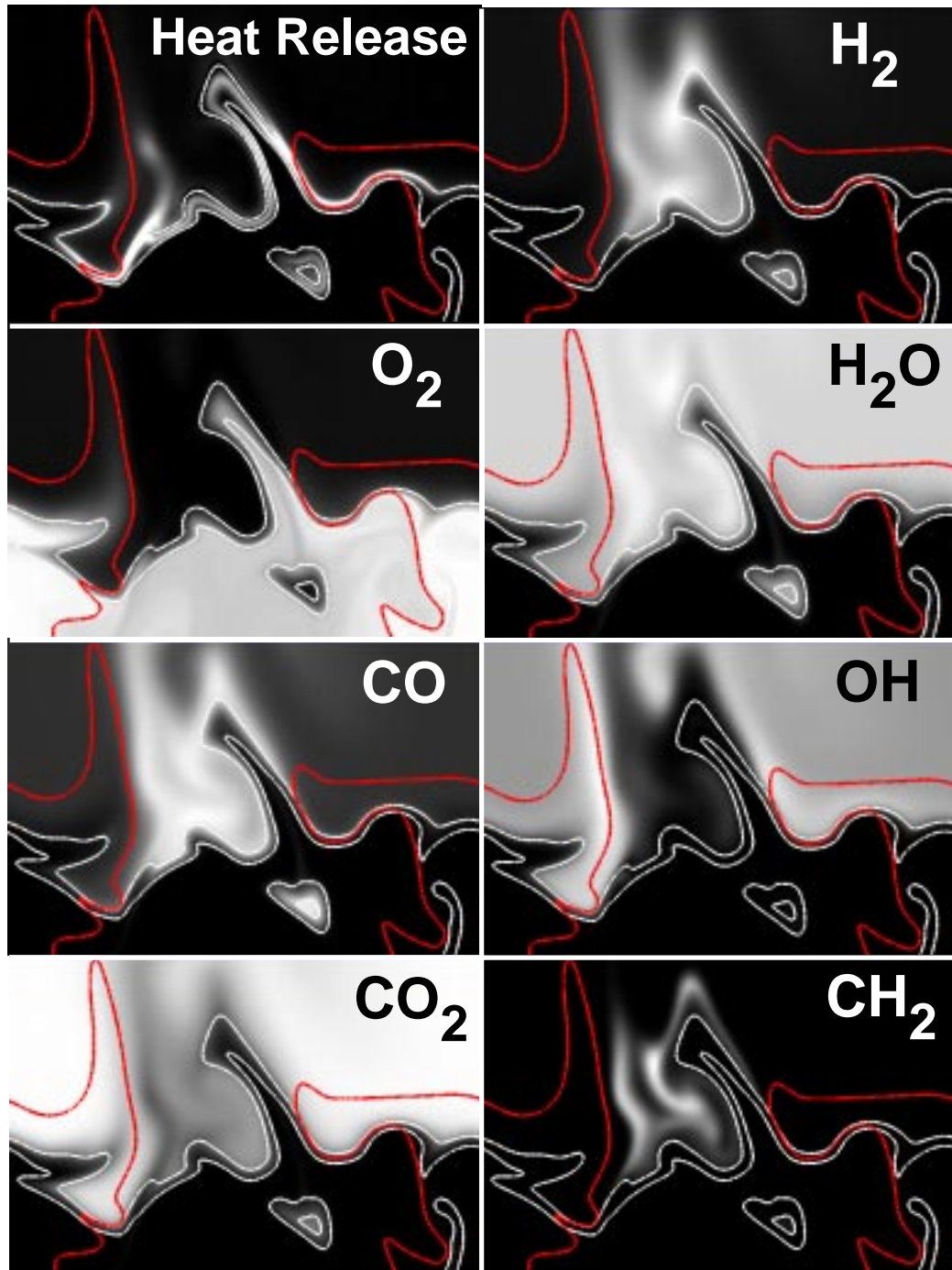


FIGURE 5. Computed two-dimensional fields at time $t/\tau_f = 3.5$ for non-homogeneous reactants (Table I). Black corresponds to (0.0) within each frame and white to the maximum value. Iso-contours of reaction progress variable (white lines: $c = 0.1$ and $c = 0.9$, Eq. 8) and stoichiometric mixture fraction (dark line: $z_{C+H} = z_{C+H_{st}} = 0.06095$, Eq. 6) are superposed. Heat release: $\dot{\omega}_Q$ (Eq. 4) (0.24 max). Y_{O_2} : (0.233 max). Y_{CO} : (0.140 max). Y_{CO_2} : (0.142 max). Y_{H_2} : (0.00751 max). Y_{H_2O} : (0.111 max). Y_{OH} : (0.00689 max). Y_{CH_2} : (0.000238 max).

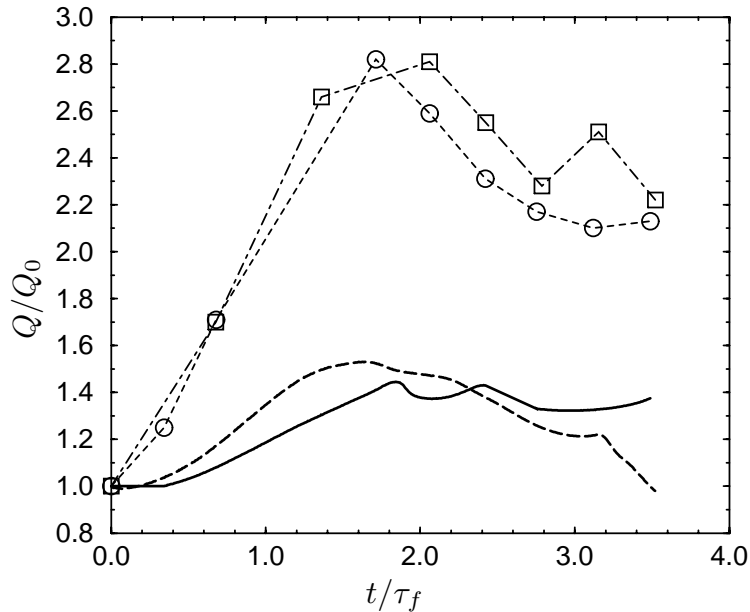


FIGURE 6. Time evolution of global heat release and flame length ($c = 0.5$ iso-contour, Eq. 8) for homogeneous stoichiometric reactants and for non-homogeneous reactants (Table I). Time is normalized by flame time τ_f (Eq. 5). Heat release and flame length are normalized by their initial values: — heat release, homogeneous; --- heat release, non-homogeneous; o --- o flame length, homogeneous; □ --- □ flame length, non-homogeneous.

And third, relatively short integration times suffice to observe effects of reactant non-homogeneity behind the primary premixed flame. For example, already at $t/\tau_f = 3.5$ the product zone behind the fuel-rich reactants is largely depleted of O_2 , O , and OH . This is a fortuitous result for numerical simulation: meaningful results concerning the secondary combustion regime can be extracted earlier in the simulations than initially thought.

The accelerating mechanism is turbulence. Counter-rotating vortex pairs pull tongues of reactants into the hot burned product region, where they quickly are consumed along their sides and highly curved tips to deposit products of rich or lean combustion behind the primary flame. Several such tongues have already appeared and burned out by the instant shown in Fig. 5, and one in the process of burning out can be seen there. This effect is exacerbated by the spatial two-dimensionality of the simulations.

5.2 The primary premixed flame

Time evolution of global heat release and flame length are plotted in Fig. 6. Flame length is computed as the length of a progress variable iso-contour ($c = 0.5$, Eq. 8); global heat release is the area integral over the entire computational box of $\dot{\omega}_Q$ (Eq. 4). Time is reported in flame-time units (Eq. 5) and heat release and flame length are normalized by their respective values for the initial one-dimensional stoichiometric flame.

Flame length increases approximately linearly in time initially, and by the latest

time shown is settling to a value corresponding to about twice the length of the initial planar stoichiometric flame. If there is any systematic difference in flame length between the homogeneous and non-homogeneous case, it is less than 10%, with the non-homogeneous case being longer. This result seems reasonable for the large-scale non-homogeneity studied here. Laminar flame speed is highest for reactants just rich of stoichiometric. Those parts of the flame penetrate deepest into the unburned reactants, while richer and leaner parts do not advance as rapidly as in the stoichiometric case, yielding a longer active flame front.

Global heat release increases much less rapidly than flame length. This is attributed to a combination of chemical kinetic and hydrodynamic strain effects. For the homogeneous case, presumably the latter dominates. It is well established that a propagating premixed flame tends to align itself with extensive strain in the tangent plane (Poinso & Haworth 1992): the net influence of turbulent straining is to reduce the heat release per unit area of flame. This effect apparently is quite strong for the conditions simulated. For the homogeneous case, the turbulent flame length is twice that of the initial planar flame, while global heat release is only about 1.4 times the laminar value. This suggests a reduction of about 30% in the mean heat release per unit flame length relative to the initial planar flame.

For non-homogeneous reactants, the global heat-release behavior combines turbulent straining and chemical kinetic effects. Global heat release increases initially at a rate that is systematically higher than that of the homogeneous stoichiometric flame; this is consistent with the transient one-dimensional results of Section 4.3. As the flame adjusts to the reactant non-homogeneity, global heat release drops dramatically so that by the end of the simulation, it is below that of the initial planar stoichiometric flame.

Heat-release profiles in the fuel-rich region are double-peaked along a direction normal to a progress variable iso-contour (Fig. 5a); between the peaks, the local heat-release rate is negative. The progress variable iso-contour $c = 0.9$ neatly tracks the heat-release valley through the fuel-rich region, and follows close to the heat-release peak for locally lean-to-stoichiometric mixtures. The $c = 0.9$ iso-contour coincides roughly with the temperature iso-contour $T \approx 1,700$ K. Normalized temperature is less satisfactory than propane mass fraction as a progress variable for non-homogeneous reactants, as temperature does not increase monotonically.

5.3 Secondary reaction

To isolate information related to post-primary combustion, it suffices to condition on a near-unity value of the reaction progress variable. Here $c > c^* = 0.999$ defines the zone of secondary reaction. Turbulent combustion closures are assessed to determine which have the most potential for modeling the secondary heat-release process (R_{F_p} in the skeletal model of Eq. 2). The approach is to analyze the mean chemical source terms $\langle \dot{\omega}_\alpha(\underline{Y}, T) \rangle_{c > c^*}$ and $\langle \dot{\omega}_Q(\underline{Y}, T) \rangle_{c > c^*}$ of Eqs. (3) and (4).

5.3.1 Chemical composition

Qualitative insight can be gained by examining the computed two-dimensional fields of Fig. 5. As for the steady stoichiometric one-dimensional laminar flame,

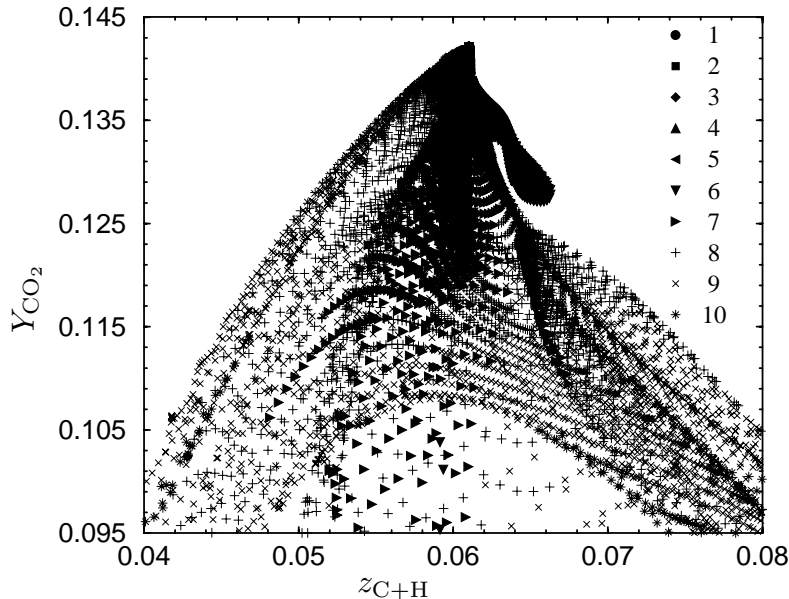


FIGURE 7. Scatter plot of Y_{CO_2} versus mixture fraction $z_{\text{C+H}}$ and dissipation rate $\log(\chi_{\text{C+H}}/(2D))$ in the post-primary-flame gases ($c > c^* = 0.999$, Eq. 8). Dissipation is ‘binned’ into ten uniformly-spaced intervals from $\min\{\log(\chi_{\text{C+H}}/(2D))\}$ to $\max\{\log(\chi_{\text{C+H}}/(2D))\}$, 1 being the lowest values of $\chi_{\text{C+H}}/(2D)$ and 10 being the highest.

species H_2O_2 and HO_2 appear along the leading edge of the turbulent flame. Progressively smaller hydrocarbon fragments mark the conversion from reactants towards products in the fuel-rich region, with only the smallest (CH and CH_2) penetrating noticeably behind the $c = 0.9$ iso-contour. Beyond three-to-four flame thicknesses behind the primary premixed flame, the only remaining fuel fragments are CO and H_2 .

5.3.2 Laminar diffusion flamelet model

Laminar flamelet theory (Peters 1984) provides an approach for decoupling detailed chemical kinetics from hydrodynamics in modeling non-premixed turbulent reacting flows. It is hypothesized that chemical reaction occurs primarily in a thin sheet that is anchored at the stoichiometric surface $z = z_{st}$. Through a formal transformation, the spatial and temporal variations of the chemical composition fields in the turbulent flow are made implicit through their dependence on mixture fraction $z(\underline{x}, t)$ and its dissipation rate $\chi(\underline{x}, t) = 2D\nabla z \cdot \nabla z$ (D being molecular diffusivity of z). A necessary, but not sufficient, condition for flamelet combustion can be expressed as,

$$Y_\alpha(\underline{x}, t) = Y_\alpha(z(\underline{x}, t), \chi(\underline{x}, t)) . \quad (9)$$

That is, the local chemical composition should be a unique function of the local mixture fraction and its dissipation rate. A second and more restrictive condition is that the functional dependence expressed in Eq. (9) be the same in the turbulent flame as in an archetypical laminar diffusion flame - usually taken to be a steady laminar counterflow diffusion flame. Only the first condition is examined here.

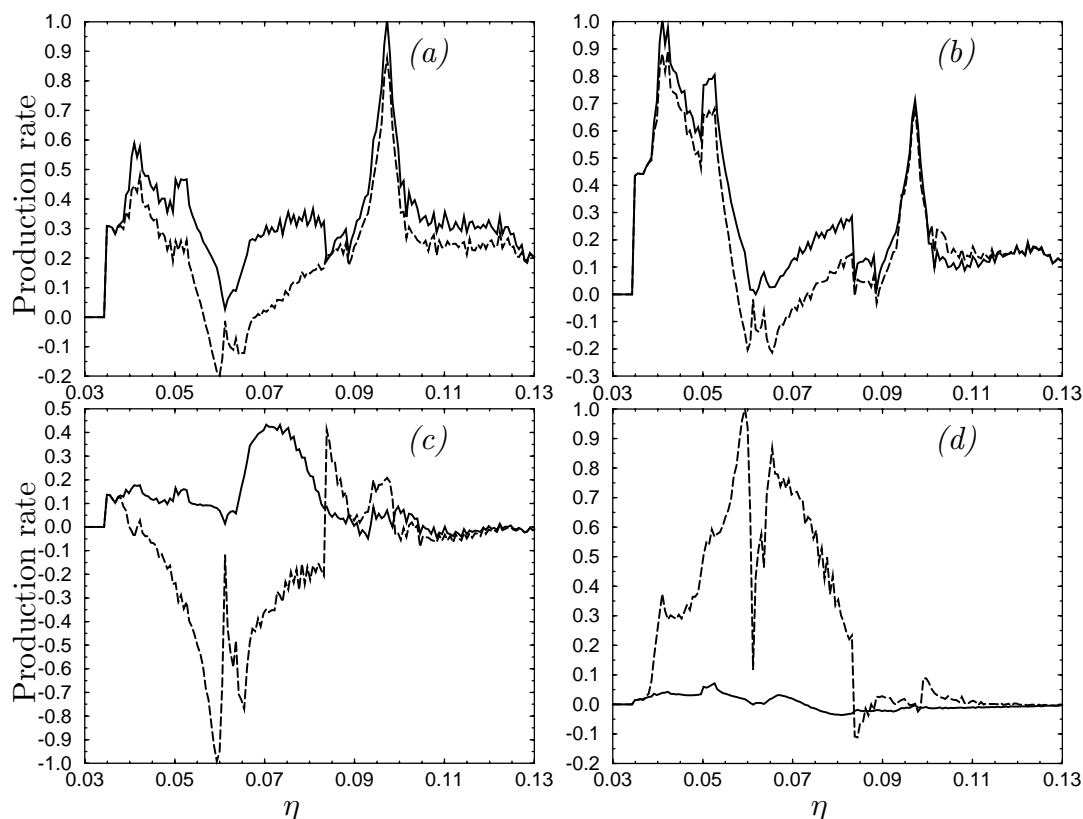


FIGURE 8. Quantities relevant to a first-order CMC model: — $\langle \dot{\omega}_\alpha(\underline{Y}, T) | z = \eta \rangle$; ---- $\dot{\omega}_\alpha(\langle \underline{Y} | z = \eta \rangle, \langle T | z = \eta \rangle)$. Mean quantities are conditioned on $c > c^* = 0.999$. The ordinate is normalized by the maximum value for each frame. a) Heat release rate. b) Chemical production rate of CO_2 . c) Chemical production rate of H_2O . d) Chemical production rate of OH .

In Fig. 7, we plot the local mass fraction of a major product species (CO_2) as a function of the local mixture fraction z_{C+H} with $\chi_{C+H}/(2D)$ as a parameter. If the combustion corresponded to a simple laminar diffusion flamelet regime, then for a given value of z_{C+H} , Y_{CO_2} would increase monotonically with decreasing χ_{C+H} . Figure 7 would display a ‘rainbow’ structure with $\chi_{C+H} = 0$ defining the upper boundary; and moving downward, successive parallel bands would correspond to increasing values of χ_{C+H} . No such pattern is evident. Nevertheless, there does appear to be some structure to this scatter plot (*e.g.*, the roughly horizontal stripes with monotonic variation in χ_{C+H}). This suggests that more sophisticated flamelet models that include conditioning variables, time-dependency (Haworth *et al.* 1988), or partial premixing of fuel and oxidizer might be appropriate.

5.3.3 Conditional moment closure (CMC) model

In conditional moment closure (CMC) (Bilger 1993), one considers conditionally averaged transport equations where the conditioning variable(s) is (are) chosen to be one(s) on which the chemical production terms are expected to have a strong dependence. Mixture fraction is, presumably, the single most appropriate conditioning

variable for non-premixed combustion.

A ‘first-order’ CMC hypothesis is that the conditional average of a chemical production term $\langle \dot{\omega}_\alpha(\underline{Y}, T) | z = \eta \rangle$ is equal to the chemical production rate evaluated using the conditionally averaged composition $\langle \underline{Y} | z = \eta \rangle$ and temperature $\langle T | z = \eta \rangle$:

$$\langle \dot{\omega}_\alpha(\underline{Y}, T) | z = \eta \rangle = \dot{\omega}_\alpha(\langle \underline{Y} | z = \eta \rangle, \langle T | z = \eta \rangle) , \quad (10)$$

and similarly for heat release. Here the notation $\langle Q | z = \eta \rangle$ denotes the mean value of Q conditioned on the mixture fraction z having the value η . The unconditional mean is recovered by integrating over the probability density function (pdf) of z , $f_z(\eta)$,

$$\begin{aligned} \langle \dot{\omega}_\alpha \rangle &= \int \langle \dot{\omega}_\alpha(\underline{Y}, T) | z = \eta \rangle f_z(\eta) d\eta , \\ \langle \dot{\omega}_\alpha \rangle_{CMC} &\equiv \int \dot{\omega}_\alpha(\langle \underline{Y} | z = \eta \rangle, \langle T | z = \eta \rangle) f_z(\eta) d\eta . \end{aligned} \quad (11)$$

The first-order CMC model is evaluated by comparing the actual and CMC mixture-fraction-conditioned means (left- and right-hand sides of Eq. 10, respectively; Fig. 8). Here the mixture fraction z_{C+H} has been used. First-order CMC captures the general shapes of the mixture-fraction-conditioned mean production rates for CO, CO₂, and heat release but not for H₂, H₂O, and most radical species. This is consistent with the expectation that the kinetics of CO₂ production dominates the secondary heat release. In classic turbulent diffusion flames, heat release and species production rates peak close to the stoichiometric value of mixture fraction. That is not the case here: most of the post-primary stoichiometric mixture in the present configuration corresponds to products of stoichiometric premixed combustion.

6. Next steps

While all results reported herein must be regarded as preliminary, significant progress has been made towards simulating non-homogeneous turbulent combustion in a specific parameter range of interest and towards understanding and modeling this combustion regime. Three principal issues remain to be addressed before definitive conclusions can be drawn: further work is needed on the chemical mechanism to strike a satisfactory balance between accuracy and computational efficiency on the fuel-rich side of stoichiometric; computations must be extended to larger computational domains (a minimum of one-centimeter square) to allow the simulation of turbulence length scales up to 2 mm; and, computations should be integrated longer in time (a minimum of five-to-ten τ_f 's) to ensure that results are free from the influence of initial conditions.

Acknowledgments

The first author thanks Mr. Nick Gallopoulos of the GM R&D Center for his continuing support of fundamental research and the opportunity to participate in this program. Several other GM personnel contributed to the success of this project: Mr. Mark Huebler assisted with customized post-processing software; and technical

discussions with Drs. Tom Sloane, Mike Drake, and Sherif El Tahry helped to guide this study. Dr. Markus Baum of NEC provided technical assistance in the use of NTMIX-CHEMKIN. Computational resources were generously provided by CERFACS. Finally, we thank the CTR organizers, hosts, and fellow visiting researchers for a stimulating and productive four weeks: in particular, Professor Parviz Moin and our CTR host Dr. W. Kendal Bushe.

REFERENCES

- BAUM, M. 1994 Etude de l'allumage et de la structure des flammes turbulentes. *Ph.D. Thesis*, Ecole Centrale.
- BAUM, M., POINSOT, T. J., HAWORTH, D. C., & DARABIHA, N. 1994 Direct numerical simulation of $H_2/O_2/N_2$ flames with complex chemistry in two-dimensional turbulent flows. *J. Fluid Mech.* **281**, 1-32.
- BILGER, R. W. 1993 Conditional moment closure for turbulent reacting flow. *Phys. Fluids A*. **5**, 436-444.
- BLINT, R. J. 1988 Flammability limits for exhaust gas diluted flames. *Twenty-Second Symposium (International) on Combustion*. (The Combustion Institute, Pittsburgh PA), 1547-1554.
- BLINT, R. J. 1991 Stretch in premixed laminar flames under IC engine conditions. *Combust. Sci. Tech.* **75**, 115-127.
- BLINT, R. J. & TSAI, P.-H. 1998 C_3H_8 -air- N_2 laminar flames calculated for stratified IC engine conditions. *Twenty-Seventh Symposium (International) on Combustion*. (The Combustion Institute, Pittsburgh PA), Poster W1E18.
- BOUDIER, P., HENRIOT, S., POINSOT, T., & BARITAUD, T. 1992 A model for turbulent flame ignition and propagation in spark ignition engines. *Twenty-Fourth Symposium (International) on Combustion*. (The Combustion Institute, Pittsburgh PA), 503-510.
- CHEN, J. H. & IM, H. G. 1998 Correlation of flame speed with stretch in turbulent premixed methane/air flames. *Twenty-Seventh Symposium (International) on Combustion*. (The Combustion Institute, Pittsburgh PA), to appear.
- EL TAHRY, S. H. 1990 A turbulent combustion model for homogeneous charge engines. *Combust. Flame*. **79**, 122-140.
- EL TAHRY, S. H. 1997 Personal communication.
- GRAN, I. R., ECHEKKI, T., & CHEN, J. H. 1996 Negative flame speed in an unsteady 2-D premixed flame: a computational study. *Twenty-Sixth Symposium (International) on Combustion*. (The Combustion Institute, Pittsburgh PA), 323-329.
- HAWORTH, D. C., DRAKE, M. C., POPE, S. B., & BLINT, R. J. 1988 The importance of time-dependent flame structures in stretched laminar flamelet models for turbulent jet diffusion flames. *Twenty-Second Symposium (International) on Combustion*. (The Combustion Institute, Pittsburgh PA), 589-597.

- HAWORTH, D. C. & POINSOT, T. J. 1992 Numerical simulations of Lewis number effects in turbulent premixed flames. *J. Fluid Mech.* **244**, 405-436.
- HÉLIE, J. & TROUVÉ, A. 1998 Turbulent flame propagation in partially premixed combustion. *Twenty-Seventh Symposium (International) on Combustion*. (The Combustion Institute, Pittsburgh PA), to appear.
- HILKA, M., VEYNANTE, D., BAUM, M., & POINSOT, T. 1995 Simulation of flame-vortex interactions using detailed and reduced chemical kinetics. *Tenth Symposium on Turbulent Shear Flows*. Pennsylvania State University.
- IM, H. G., CHEN, J. H., & LAW, C. K. 1998 Ignition of hydrogen/air mixing layer in turbulent flows. *Twenty-Seventh Symposium (International) on Combustion*. (The Combustion Institute, Pittsburgh PA), to appear.
- KEE, R. J., MILLER, J. A., & JEFFERSON, T. H. 1980 Chemkin: a general-purpose, problem-independent, transportable fortran chemical-kinetics package. *Sandia Tech. Rep. SAND80-8003*.
- KEE, R. J., WARNATZ, J., & MILLER, J. A. 1983 A fortran computer code package for the evaluation of gas-phase viscosities, conductivities, and diffusion coefficients. *Sandia Tech. Rep. SAND83-8209*.
- KHALIGHI, B., EL TAHRY, S. H., HAWORTH, D. C., & HUEBLER, M. S. 1995 Computation and measurement of flow and combustion in a four-valve engine with intake variations. *SAE Paper No. 950287*.
- KRIEGER, R. B., SIEWERT, R. M., PINSON, J. A., GALLOPOULOS, N. E., HILDEN, D. L., MONROE, D. R., RASK, R. B., SOLOMON, A. S. P., & ZIMA, P. 1997 Diesel engines: one option to power future personal transportation vehicles. *SAE Paper No. 972683*.
- LAI, M. C., ZHAO, F. Q., & HARRINGTON, D. L. 1997 A review of mixture preparation and combustion control strategies for spark-ignited direct-injection gasoline engines. *SAE Paper No. 970627*.
- LELE, S. 1992 Compact finite difference schemes with spectral-like resolution. *J. Comput. Phys.* **103**, 16-42.
- PETERS, N. 1984 Laminar diffusion flamelet models in non-premixed turbulent combustion. *Prog. Energy Combust. Sci.* **10**, 319-339.
- POINSOT, T., VEYNANTE, D., TROUVÉ, D., & REUTSCH, G.R. 1996 Turbulent flame propagation in partially premixed flames. *Proceedings of the Summer Program*, Center for Turbulence Research, NASA Ames/Stanford University, 111-136.
- URNS, S. R. 1996 *An Introduction to Combustion*. McGraw-Hill, Inc., New York.
- WARNATZ, J. 1981 The structure of laminar alkane-, alkene-, and acetylene flames. *Eighteenth Symposium (International) on Combustion*. (The Combustion Institute, Pittsburgh PA), 369-384.